Tuning the photocatalytic activity of TiO_2 nanoparticles by ultrathin SiO_2 films grown by low-temperature atmospheric pressure atomic layer deposition

Guo, Jing; Benz, Dominik; Doan Nguyen, Thao Trang; Nguyen, Phuc Huy; Thi Le, Thanh Lieu; Nguyen, Hoai Hue; La Zara, Damiano; Liang, Bin; Hintzen, Hubertus T.(Bert); van Ommen, J. Ruud

DOI
10.1016/j.apsusc.2020.147244

Publication date
2020

Document Version
Final published version

Published in
Applied Surface Science

Applied Surface Science 530 (2020) 147244

Contents lists available at ScienceDirect

Applied Surface Science

journal homepage: www.elsevier.com/locate/apsusc

Full Length Article

Tuning the photocatalytic activity of TiO_2 nanoparticles by ultrathin SiO_2 films grown by low-temperature atmospheric pressure atomic layer deposition

Jing Guo[a,b,c], Dominik Benz[a], Thao-Trang Doan Nguyen[d], Phuc-Huy Nguyen[d], Thanh-Lieu Thi Le[d], Hoai-Hue Nguyen[e,f], Damiano La Zara[a], Bin Liang[b], Hubertus T. (Bert) Hintzen[g], J. Ruud van Ommen[a], Hao Van Bui[e,f,*]

[a] Product & Process Engineering, Department of Chemical Engineering, Faculty of Applied Sciences, Delft University of Technology, 2629 HZ Delft, the Netherlands
[b] Multi-phase Mass Transfer & Reaction Engineering Lab, College of Chemical Engineering, Sichuan University, 610065 Chengdu, China
[c] Shanxi Province Key Laboratory of Higee-Oriented Chemical Engineering, College of Chemical Engineering and Technology, North University of China, Taiyuan, Shanxi 030051, China
[d] Faculty of Natural Sciences, Quy Nhon University, 170 An Duong Vuong, Quy Nhon City 590000, Viet Nam
[e] Faculty of Electrical and Electronic Engineering, Phenikaa University, Yen Nghia, Ha-Dong District, Hanoi 12116, Viet Nam
[f] Faculty of Materials Science and Engineering, Phenikaa University, Yen Nghia, Ha-Dong District, Hanoi 12116, Viet Nam
[g] Group Luminescent Materials, Section Fundamental Aspects of Materials and Energy, Faculty of Applied Sciences, Delft University of Technology, 2629 HZ Delft, the Netherlands

ARTICLE INFO

Keywords:
TiO_2/SiO_2 core/shell nanoparticles
Photocatalysts
Low-temperature deposition
Atmospheric pressure atomic layer deposition
Ultrathin SiO_2 coating
Fluidized bed reactor

ABSTRACT

We employed atomic layer deposition (ALD) to deposit ultrathin SiO_2 layers on P25 TiO_2 nanoparticles to fabricate TiO_2/SiO_2 core/shell nanostructures. The ALD process was carried out in a fluidized bed reactor working at atmospheric pressure using $SiCl_4$ and H_2O as precursors, enabling the deposition of SiO_2 at 100 °C with the ability to control the thickness at the sub-nanometer level. By controlling the thickness of the SiO_2 in a very narrow range, i.e., below 2 nm, the photocatalytic activity of TiO_2 can be tuned. In particular, an enhancement was obtained for the SiO_2 layers with a thickness below 1.4 nm, in which the layer with a thickness of about 0.7 nm exhibited the highest photocatalytic activity; for SiO_2 layers thicker than 1.4 nm, the photocatalytic activity was strongly suppressed. The photocatalytic activity enhancement and the degradation mechanism of RhB by the TiO_2/SiO_2 photocatalysts were investigated by combining X-ray photoelectron spectroscopy, UV–Vis absorption spectroscopy, photoluminescence spectroscopy and the aid of charge carrier and radical scavengers. Our findings have revealed an improvement of photogenerated charge separation due to the SiO_2 coating and the dominating role of hydroxyl radicals in the degradation of RhB.

1. Introduction

For a few decades since Fujishima and Honda discovered the photocatalytic splitting of water on TiO_2 electrodes [1], enormous efforts have been devoted to the development of TiO_2 photocatalysis. Owing to its excellent photocatalytic properties, high structural and chemical stabilities, low environmental impact, abundance in nature, and especially its suitable flat band potential for various redox reactions, TiO_2 has been widely used in various applications in environmental and energy-related fields, such as air purification, water treatment and hydrogen production [2–7]. However, due to its large band gap (i.e., ~3.2 eV), TiO_2 does not harvest efficiently sunlight that provides the highest photon flux in the visible and infrared regions [8]. In addition, the rapid recombination of photogenerated electrons and holes is a limiting factor to achieve high photocatalytic efficiencies [6,9]. Therefore, to improve light harvesting and to reduce charge recombination, electronic structure and surface properties of TiO_2 are usually modified.

The electronic modification of TiO_2 is commonly realized by doping the host material with other elements to form energy levels in the band gap of TiO_2 [3,10–13]. This consequently reduces the bandgap and enables the absorption of photons with lower energies [6,14–16]. In

* Corresponding author at: Faculty of Electrical and Electronic Engineering, Phenikaa University, Yen Nghia, Ha-Dong District, Hanoi 12116, Viet Nam (H. Van Bui).
E-mail address: hao.buivan@phenikaa-uni.edu.vn (H. Van Bui).

https://doi.org/10.1016/j.apsusc.2020.147244
Received 17 October 2019; Received in revised form 14 June 2020; Accepted 10 July 2020
Available online 15 July 2020
0169-4332/

contrast, surface modification commonly promotes the charge transfer between the TiO_2 and the deposited materials, which can reduce the charge recombination [14]. In this case, the surface of TiO_2 is engineered by coupling with a thin film or nanoclusters of other materials. Due to their high catalytic activities, noble metals are most popularly used [17–20]. In addition to promoting the electron transfer due to their lower Fermi levels with respect to the conduction band of TiO_2 [21–23], noble metals can also act as co-catalysts, providing further catalytic enhancement [14]. For instance, the surface modification of TiO_2 nanoparticles by Pt nanoclusters could significantly improve the photocatalytic activity of TiO_2 toward the degradation of acid blue 9 [24]. An enhancement of photocatalytic performance was also observed for the TiO_2 modified with nanoclusters of Au, Ag and Cu [17,25–27]. Nevertheless, the use of noble metal may reduce the stability of the catalysts due to the oxidation at the metal/TiO_2 interface when exposed to UV-irradiation. This can create electron-hole recombination centers that affect the photocatalytic efficiency [28]. In addition, due to their high cost, the use of noble metals is not desirable. Therefore, the surface modification of TiO_2 by metal oxides such as CuO, Cu_2O, Fe_2O_3, CeO_2, MnO_2 and MgO has recently been more attractive [25,29–34].

Given its large band gap (~9 eV), silicon dioxide (SiO_2) is an excellent dielectric that has been a key material in the microelectronic industry. The good electrically insulating nature of SiO_2 also makes it the material of choice for mitigating the photocatalytic activity of TiO_2 [35–37]. This is due to the fact that a thin SiO_2 layer can effectively block the transport of photogenerated electrons and holes to the catalyst surface, diminishing the photocatalytic reactions [35]. Nevertheless, many studies have also shown that the coupling with SiO_2 can enhance the photocatalytic activity of TiO_2, which has been utilized in various fields, such as degradation of pollutants [38–47] and bacteria [48,49], heavy metal removal [50], CO_2 capture [51] and other applications [52–57]. Generally, the enhancement or suppression of photocatalytic activity strongly depends on the concentration (i.e., in the case of TiO_2-SiO_2 mixture) or the thickness (i.e., in the case of TiO_2/SiO_2 core/shell structure) of SiO_2. For example, for the TiO_2/SiO_2 core/shell structure, a thin layer of SiO_2 with a thickness of about 1–2 nm can effectively diminish the photocatalytic activity of TiO_2 [37,58]. Therefore, in order to achieve an enhancement, a thinner layer is needed. This requires a synthesis method that allows to control the thickness of the coating layer at the sub-nanometer level. In this regard, atomic layer deposition (ALD) is an excellent candidate. This is a gas-phase deposition technique that allows to control the amount of deposited material down to the atomic scale, which has been utilized for the deposition of various materials [59,60].

In this work, we employed ALD to deposit ultrathin SiO_2 layers on P25 TiO_2 nanoparticles to fabricate TiO_2/SiO_2 core/shell nanostructures and investigate their photocatalytic properties. The SiO_2 ALD process was carried out in a fluidized bed reactor (FBR) operating at atmospheric pressure using silicon tetrachloride ($SiCl_4$) as the precursor and H_2O as the co-reactant. Such a process not only enabled the deposition of SiO_2 at a temperature as low as 100 °C, but also provided the ability to control the thickness of the SiO_2 at the sub-nanometer level. The photocatalytic properties of the TiO_2/SiO_2 photocatalysts were investigate by the degradation of Rhodamine B (RhB) solution under UV-light irradiation. We observed that the photocatalytic activity of the TiO_2 was significantly enhanced by depositing a SiO_2 layer with a thickness of below 1.4 nm; for a thicker layer, the photocatalytic activity was strongly suppressed. By combining X-ray photoelectron spectroscopy, UV–Vis absorption spectroscopy, photoluminescence spectroscopy and the aid of charge carrier and radical scavengers, insights into the photocatalytic activity enhancement and the degradation mechanism of RhB by the TiO_2/SiO_2 photocatalysts were achieved, which emphasized the improvement of photogenerated charge separation due to the SiO_2 coating and the dominating role of hydroxyl radicals in the degradation of RhB.

2. Experimental methods

2.1. Preparation of TiO_2/SiO_2 core/shell photocatalysts

The deposition of SiO_2 on TiO_2 nanoparticles was carried out in a fluidized bed reactor (FBR) operating at atmospheric pressure, as described elsewhere [61]. Degussa P25 TiO_2 (mean diameter of 21 nm and specific surface area of 54 $m^2\ g^{-1}$) was purchased from Evonik Industries (Hanau, Germany). Silicon tetrachloride ($SiCl_4$) contained in a stainless steel bubbler was provided by Akzo Nobel HPMO (Amersfoort, the Netherlands). Nitrogen (99.999 vol%) was used as the carrier gas. For each experiment, 1.5 g of powder was used. The powder is fluidized by an N_2 gas flow of 0.5 L min^{-1}, which was introduced through the distributor plate placed at the bottom of the glass column. An ALD cycle consisted of alternating exposures of the TiO_2 powder to $SiCl_4$ vapor (1 min), followed by an N_2 purging step (3 min), the deionized water vapor (3 min), and finally an N_2 purging of 8 min. The deposition temperature was set at 100 °C. During the deposition, a temperature variation of ± 5 °C was observed.

2.2. Characterization

The morphology of the TiO_2/SiO_2 particles was characterized by transmission electron microscopy (TEM) using a JEOL JEM1400 transmission electron microscope. X-ray photoelectron spectroscopy (XPS) was employed to investigate elemental compositions and bonding states of the TiO_2/SiO_2 catalysts using a ThermoFisher K-Alpha system (photon energy of 1486.7 eV). The peak positions were calibrated by using the C 1s peak at 284.8 eV as the reference. The UV–Vis diffuse reflectance spectra (DRS) were recorded using a PerkinElmer-Lambda 900 spectrometer. The photoluminescence spectra of the catalysts were investigated using a Horiba Jobin Yvon spectrometer equipped with a 450 W xenon discharge lamp as the excitation source.

The atomic concentration of the deposited SiO_2 was determined using instrumental neutron activation analysis (INAA). For each measurement, 100 mg powder was loaded into high purity polyethylene capsules. The samples and a reference sample were irradiated at a constant neutron flux. All reactors used for neutron activation employed uranium fission, which provides a neutron flux (kinetic energy less than 0.5 eV) in the order of 10^{12} $cm^{-2}\ s^{-1}$. Upon irradiation, a neutron can be absorbed by the target nucleus (i.e., Si), forming a radioactive nucleus. The nuclear decay of the radioactive nuclei produce Gamma rays, which can be detected by the INAA detectors, from which the Si loading was determined.

The specific surface area (SSA) of the powder was determined by BET method using a Micromeritics Tristar II at 77 K. For each measurement, 160 mg of the powder was used. All the samples were annealed in N_2 at 150 °C for 16 h prior to the measurements. Data analysis was performed using Microactive software V3.02. The BET SSA was determined by fitting of data points in the P/P_0 = 0.05–0.225 region.

The photodegradation of Rhodamine B (RhB) in aqueous solution was used to evaluate the photocatalytic activity of the TiO_2/SiO_2 photocatalysts. In each experiment, 10 mg of the catalyst was added to 80 mL RhB solution (RhB concentration of 10 mg L^{-1}) contained in a 200-ml glass beaker (diameter of 8 cm). The suspension was continuously stirred in the dark for 60 min to obtain the adsorption/desorption equilibrium, which was then exposed to UV-radiation generated by a mercury lamp for different exposure times. After separating the solid catalyst by centrifuging, the solution was analyzed by UV–visible spectroscopy using a Jenway's 6800 double beam spectrophotometer to determine the RhB residual concentration.

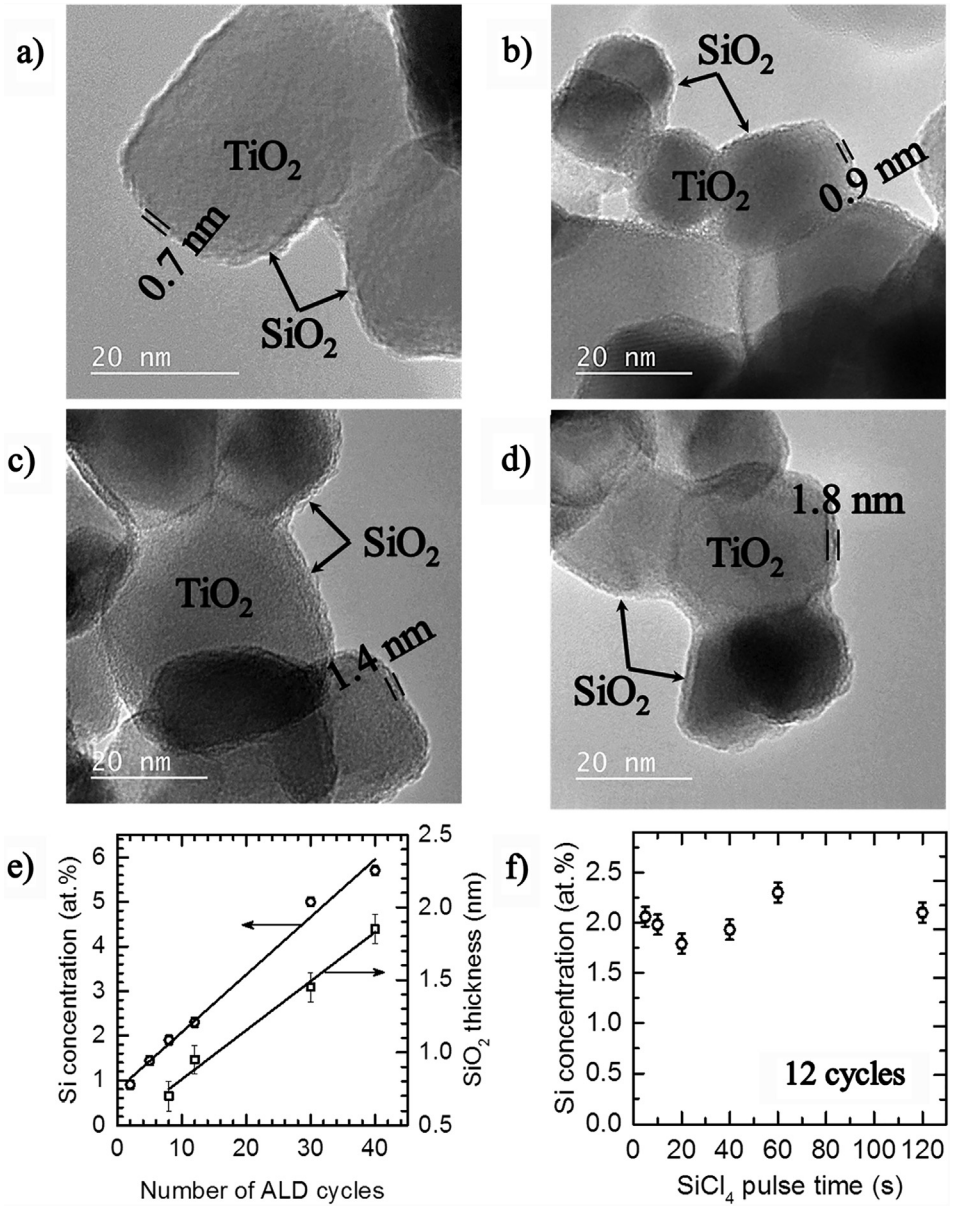

Fig. 1. TEM images of TiO_2 nanoparticles coated with SiO_2 films grown at 100 °C for 8 cycles (a), 12 cycles (b), 30 cycles (c) and 40 cycles (d). The SiO_2 film thickness (□) and the Si atomic concentration (○) as a function of the number of cycles are plotted in (e). The plot in (f) shows the Si atomic concentration obtained for 12 ALD cycles in which the $SiCl_4$ pulse time is varied from 5 to 120 s while the pulse time of H_2O vapor is fixed at 300 s.

3. Results and discussion

3.1. Morphology, structure and elemental composition of the TiO_2/SiO_2 photocatalysts

The reactions between $SiCl_4$ and H_2O in ALD of SiO_2 are based on the ligand exchange between the functional groups, i.e., −Cl and −OH, on the surface, which requires a relatively high temperature, typically in the range of 300–420 °C [62–64]. For lower deposition temperatures, the presence of a catalyst, such as ammonia (NH_3) or pyridine (C_5H_5N), is commonly needed [65,66]. Nevertheless, the $SiCl_4/H_2O$ ALD process carried out in a fluidized bed reactor operating at atmospheric pressure in this work enabled the growth of SiO_2 at 100 °C, which is significantly lower than the deposition temperature reported in the literature [62–64]. This is indicated by the TEM images presented in Fig. 1a–d, which show the TiO_2/SiO_2 nanoparticles with a core/shell structure. From the TEM images, the thickness of the SiO_2 layer is determined, whereas the Si atomic concentration (Si at.%) is measured by INAA. The plots of SiO_2 thickness and Si at.% as a function of the number of ALD cycles exhibit a linear dependence (Fig. 1e) that represents the linear-growth regime of ALD [60]. In this regime, a growth-per-cycle (GPC) of approximately 0.5 Å is obtained, which is slightly lower than the GPC of the SiO_2 ALD reported in the literature (i.e., 0.7–1.1 Å) [62,63]. In addition, the constancy of the GPC obtained for different $SiCl_4$ exposure times (i.e., from 5 s to 120 s) shown in Fig. 1f reflects the self-saturating behavior of ALD [60]. This self-limiting behavior in combination with the linear-growth provides the ability to control the thickness of the SiO_2 layer at the sub-nanometer level by controlling the number of cycles. This allows us to investigate the influence of the SiO_2 thickness at the ultrathin regime (i.e., less than 2 nm) on the photocatalytic activity of TiO_2.

The specific surface area (SSA) of the TiO_2 powders before and after coating with SiO_2 is determined by BET method. An SSA of 54.5 $m^2\,g^{-1}$ is obtained for the uncoated P25 TiO_2, which is consistent with the SSA value provided by the supplier. No considerable change is observed for the total SSA obtained for the TiO_2 powder coated with SiO_2 for

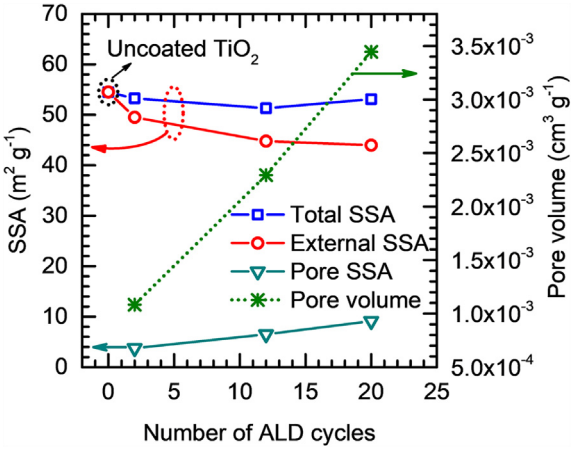

Fig. 2. The total SSA (□), micropore SSA (▽), micropore volume (*) and external SSA (○) of the TiO_2 powder coated with SiO_2 for different numbers of ALD cycles as determined by BET.

different numbers of ALD cycles, as shown in Fig. 2 (the squares). However, using the T-method [67], the analysis of the isothermal curves reveals the presence of micropores in the SiO_2 films whose volume and SSA increase with the number of cycles (Fig. 2, the stars and the triangles). The external SSA of the powders is determined from the total SSA and the SSA of the micropores, showing a slight decrease with increasing the number of ALD cycles (Fig. 2, the circles). This decrease is attributed to the increase in particle size caused by the SiO_2 coating layer.

The results obtained from the XRD characterization show the amorphous state of the SiO_2 films, even after annealing at 500 °C for 16 h (Fig. S1, Supporting Information). The XPS spectra of the C 1s, Ti 2p, O 1s and Si 2p core-levels of the uncoated TiO_2 and TiO_2/SiO_2 are presented in Fig. 3. We note that in order to eliminate the influence of the peak shift due to charging effects, the peak positions are calibrated by referencing the C − C peak of the C 1s to the binding energy (BE) of 284.8 eV (Fig. 3a) [40]. For the uncoated TiO_2, the two peaks at BE = 464.2 eV (Ti $2p_{1/2}$) and BE = 458.6 eV (Ti $2p_{3/2}$) in the top spectrum of Fig. 3b reflect doublet state of Ti(IV) 2p that arises from the spin–orbit coupling. These two peaks in conjunction with the peak at BE = 529.7 eV of O 1s (Fig. 3c, the top spectrum) represent the Ti − O bond of TiO_2 (hereafter designated as $O-_{Ti}$) [40,68,69]. The peak at BE = 457.4 eV in the Ti 2p top spectrum (Fig. 3b) could represent the Ti $2p_{3/2}$ of the Ti(III) compounds (e.g., Ti_2O_3, oxygen vacancies, etc.) [69], whereas the broad peak at 532.0 eV in the O 1s top spectrum (Fig. 3c) is attributed to the chemisorbed hydroxyl groups (i.e., OH groups) on the surface [51]. The presence of these OH groups is confirmed by the FTIR spectra (Fig. S2, Supporting Information).

For TiO_2/SiO_2, the peak at BE = 532.4 eV (O 1s, Fig. 3c) and the peak at BE = 103.0 eV (Si 2p, Fig. 3d) represent the Si − O bond (hereafter designated as $O-_{Si}$) [70,71]. The binding energy difference between the Si 2p and the O 1s of the $O-_{Si}$ bond is 429.4 eV, which is consistent with the binding energy difference of the Si − O bond of SiO_2 (i.e., 429.3–429.4 eV) [70,71]. Furthermore, after coating with SiO_2, the Ti 2p and O 1s peaks of the $O-_{Ti}$ bond exhibit remarkable shifts (i.e., 0.4 eV for Ti 2p and 0.5 eV for O 1s) toward the higher binding energy (Fig. 3b and Fig. 3c). This shift is evidence of the formation of Ti − O − Si linkages at the interface between TiO_2 and SiO_2 and arises from the difference in electron negativity between Si (1.90), Ti (1.56) and O (3.44) [40,72]. The presence of the linkages is also indicated by the peak at 531.8 eV in the O 1s spectrum (Fig. 3c) [73,74]. The XPS analyses confirm the presence of SiO_2, which is additionally supported by the FTIR spectra (Fig. S2, Supporting Information). In addition, the XPS data also demonstrated that the Si 2p and Ti 2p spectra were not affected after the photocatalytic test, which indicated a good chemical stability of the catalyst (Fig. S3, Supporting Information).

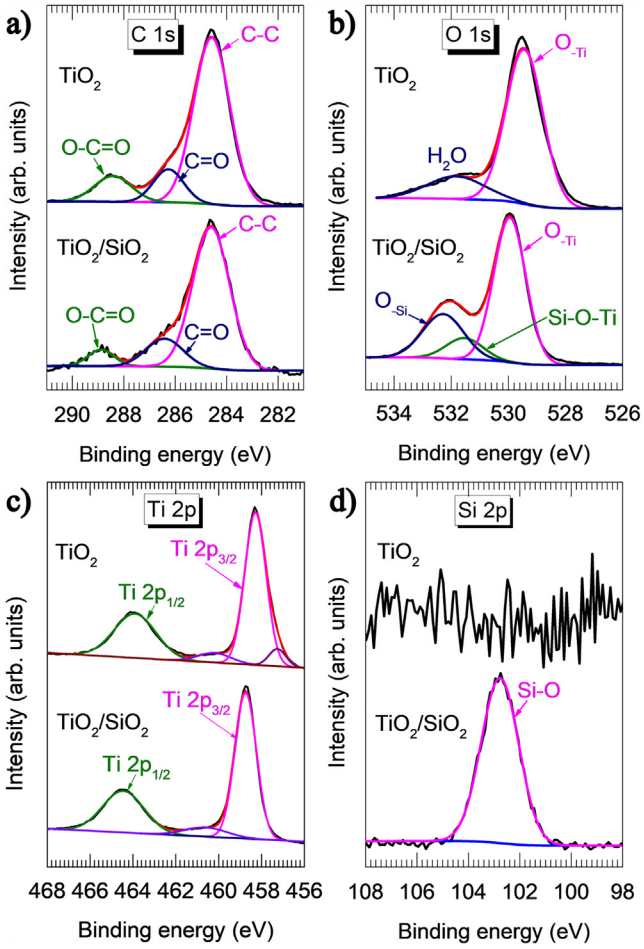

Fig. 3. Core-level XPS spectra of C 1s (a), Ti 2p (b), O 1s (c) and Si 2p (d) of the uncoated TiO_2 (top spectra) and TiO_2 coated with SiO_2 for 12 ALD cycles (bottom spectra).

3.2. Photocatalytic performance of the TiO_2/SiO_2 photocatalysts

The adsorption of RhB on the surface of the photocatalysts was examined by monitoring the change of RhB concentration during stirring the catalyst/RhB aqueous mixture in the dark before UV-light irradiation. As shown in Fig. 4a, a similar variation of the RhB concentration is observed for all samples: a rapid decrease in the first 10 min, followed by a saturation. The former is caused by the adsorption of RhB on the surface of TiO_2, whereas the latter indicates the adsorption–desorption equilibrium. No significant difference in the adsorption of RhB on uncoated TiO_2 and SiO_2-coated TiO_2 was observed, suggesting that the adsorption of RhB molecules was not enhanced by the SiO_2 layer. This is in contrast with the results reported in the pioneering work of Anderson and Bard, in which an enhanced adsorption of the organic molecules on the catalyst surface due to SiO_2 was observed [39,75]. However, the SiO_2 layer strongly altered the photodegradation of RhB under UV-light irradiation, as shown in Fig. 4b. Particularly, for the uncoated TiO_2, approximately 90% of the RhB was degraded after 30 min irradiation. For the TiO_2/SiO_2 photocatalysts, the photodegradation exhibited a strong dependence on the thickness of the SiO_2 coating layer, which can be estimated by the kinetics of the photodegradation reaction described by equation [76]:

$$\ln(C_0/C) = k_{app}\cdot t, \text{ or } C = C_0\cdot\exp(-k_{app}\cdot t) \quad (1)$$

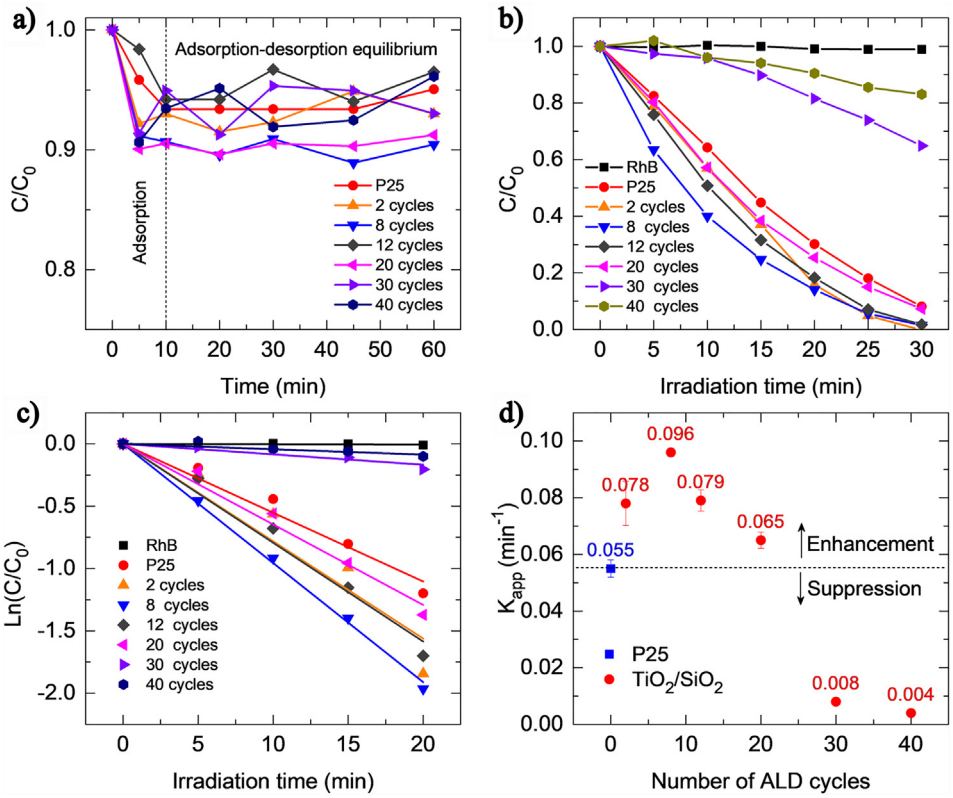

Fig 4. Adsorption behavior of RhB on TiO_2 and TiO_2/SiO_2 surface before UV irradiation (i.e., in the dark) (a), the degradation of RhB as a function of irradiation time (b) and the corresponding kinetic plots (c), from which the first-order kinetic constants were determined and plotted (d).

where k_{app} represents the degradation rate, which is commonly referred as the apparent first-order kinetic constant. The $\ln(C_0/C)$ *versus* t plots are shown in Fig. 4c, from which the k_{app} values were determined and plotted in Fig. 4d. For the uncoated TiO_2, a k_{app} of 55.2×10^{-3} min^{-1} was obtained. The coating of TiO_2 by SiO_2 initially resulted in an increase of k_{app} with increasing the number of ALD cycles, reached the maximum value of 95.6×10^{-3} min^{-1} at 8 ALD cycles (i.e., SiO_2 film thickness of about 0.7 nm). Hereafter, k_{app} gradually decreased to 64.6×10^{-3} min^{-1} for 20 ALD cycles, which was slightly higher than the k_{app} obtained for the uncoated TiO_2. A further increase of the number of cycles to 30 and 40 resulted in a rapid drop of k_{app} to 8.4×10^{-3} min^{-1} and 4.3×10^{-3} min^{-1}, respectively. The low k_{app} values achieved for 30 and 40 ALD cycles (i.e., SiO_2 thickness of 1.4 and 1.8 nm, respectively) indicate that the photocatalytic activity of TiO_2 was strongly suppressed.

3.3. Roles of photogenerated electrons, holes and radicals in the degradation of RhB by the TiO_2/SiO_2 photocatalysts

The photodegradation of organic dyes by TiO_2-based photocatalysts may be involved with a number of photocatalytic oxidation processes. Generally, under UV-light irradiation, electrons in the valence band are excited to the conduction band, generating charge carriers (i.e., electrons in the conduction band and holes in the valence band). These electrons and holes may recombine or diffuse to the catalyst surface to take part in various photocatalytic reactions. Particularly, the electrons in the conduction band can be absorbed by oxygen molecules, generating superoxide radicals ($O_2\cdot^-$) that can take part in the destruction of organic molecules [2,77,78]. The holes in the valence band can be absorbed by H_2O molecules, generating OH· radicals [77,79–81], which have been considered as the main oxidizing species for the degradation of most of organic compounds [82,83]. In this work, the role of the charge carriers and radicals in the photodegradation of RhB by the TiO_2/SiO_2 photocatalysts was investigated by using scavengers: ethylenediaminetetraacetic acid (EDTA) as the hole scavenger [84], benzoquinone as the $O_2\cdot^-$ scavenger [85], and dimethyl sulfoxide (DMSO) as the OH· scavenger [86].

Fig. 5a–c present the photodegradation of RhB by the TiO_2 coated with SiO_2 for 8 ALD cycles in the presence of the scavengers with different concentrations. On the one hand, the plots in Fig. 5a show that when EDTA was added, the photodegradation of RhB was significantly attenuated. Particularly, for an EDTA concentration of 0.05 mmol, negligible degradation was observed in the first 20 min of the irradiation, whereas for the higher EDTA concentrations the degradation was only slightly lower than the self-degradation of RhB. This indicates the key role of holes in the degradation of the dye. In contrast, in the presence of benzoquinone, the degradation of RhB by TiO_2/SiO_2 was nearly unaffected (Fig. 5b), which is also indicated by the nearly constant k_{app} values shown in Fig. 5d. As benzoquinone is a scavenger of $O_2\cdot^-$ radicals that are formed due to the reduction of dissolved O_2 by photogenerated electrons in the conduction band, the nearly unaffected degradation curves in Fig. 5b suggest the minor contribution of photogenerated electrons. This is consistent with the conclusion on the dominating role of holes obtained from the study shown in Fig. 5a. On the other hand, in the presence of DMSO, the degradation was strongly reduced (Fig. 5c). More particularly, k_{app} decreased from 95.6×10^{-3} min^{-1} (i.e., no scavenger) to 6.4×10^{-3} min^{-1} at a DMSO concentration of 2.0 mmol. Hereafter, a further increase of DMSO concentration to 3.0 mmol did not result in any considerable decrease of the degradation rate (i.e., $k_{app} = 4.7 \times 10^{-3}$ min^{-1}). The strong decrease of the degradation rate in the presence of the OH· scavenger indicates that the oxidation of RhB was mainly caused by OH· radicals.

The results show that by varying the thickness of the SiO_2 layer, the photocatalytic activity of TiO_2 can be tuned. In particular, an enhancement can be achieved by coating the TiO_2 with a SiO_2 layer thinner than 1.4 nm, in which a layer of 0.7 nm provides the highest

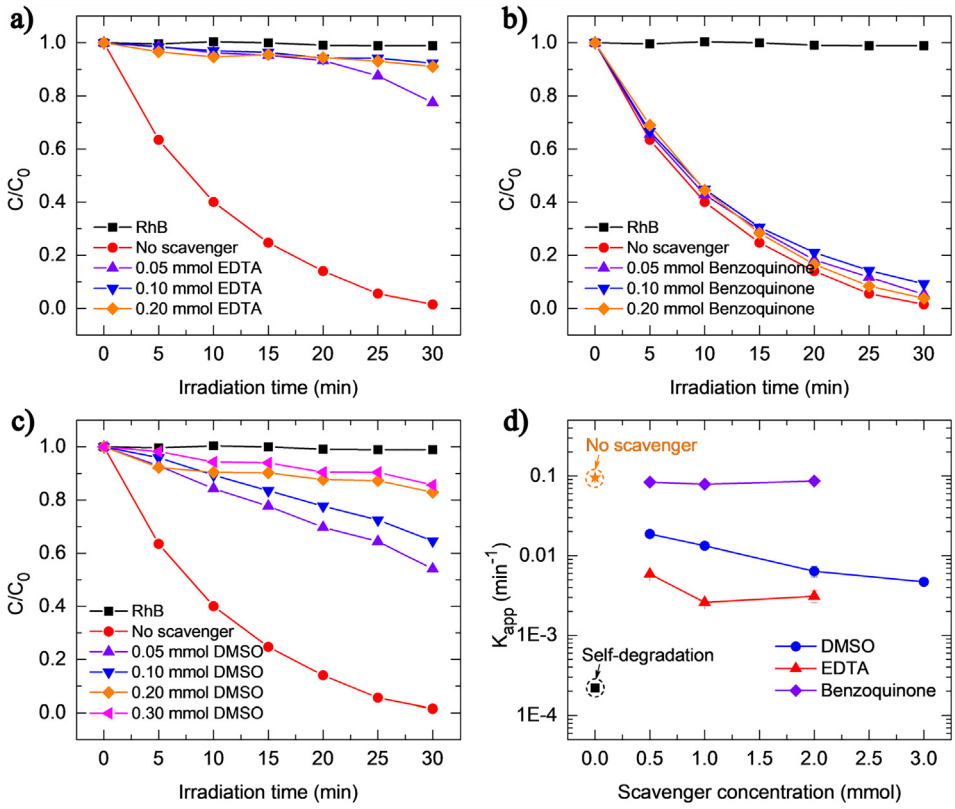

Fig 5. Photodegradation of RhB by the TiO_2 coated with SiO_2 for 8 ALD cycles in the presence of hole scavenger – EDTA (a), superoxide radical scavenger – benzoquinone (b) and hydroxyl radical scavenger – DMSO (c) with different concentrations. The plots in (d) compare the k_{app} values of the degradation processes presented in (a), (b) and (c).

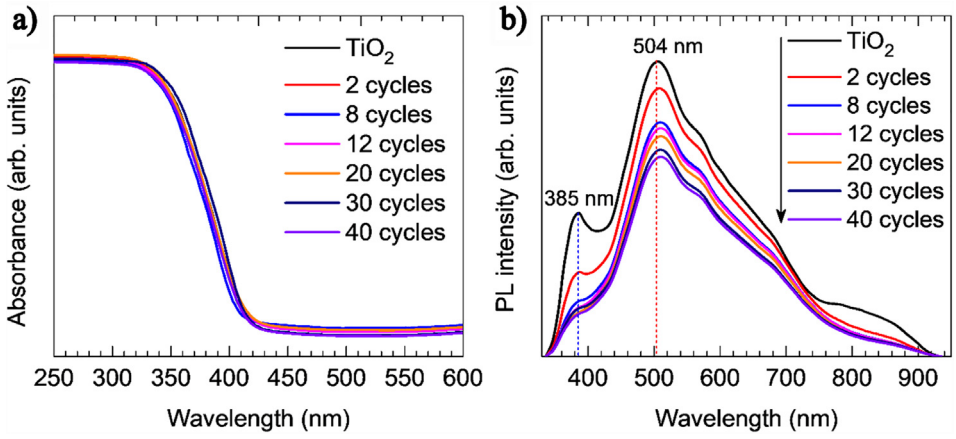

Fig. 6. UV–Vis absorption spectra (a) and photoluminescence spectra (b) of TiO_2 and TiO_2 coated with SiO_2 for different number of cycles.

photocatalytic activity. For the SiO_2 layers thicker than 1.4 nm, the photocatalytic activity of TiO_2 is significantly suppressed. The suppression of the photocatalytic activity of TiO_2 can be attributed to the insulating properties of the thicker SiO_2, which hindered the charge transport from TiO_2 to the surface [35,58]. In an attempt to explain the enhancement of photocatalytic activity of the TiO_2/SiO_2 photocatalysts with thin SiO_2 layers, we investigated the UV–Vis absorption and photoluminescence (PL) properties of the catalysts, which are presented in Fig. 6. The UV–Vis spectra in Fig. 6a show absorption edges at around 415 nm without a noticeable effect of the SiO_2 coating. However, the PL spectra shown in Fig. 6b exhibit a strong influence of the SiO_2 coating on the PL properties of the photocatalysts. Specifically, for the uncoated TiO_2, two emission peaks at around 385 nm and 504 nm were observed. The peak at 385 nm is attributed to the radiative band-to-band recombination [87], whereas the peak at 504 nm is due to the radiative recombination of the conduction band electrons with trapped holes [88]. After coating with SiO_2 for 2 and 8 ALD cycles, the PL intensity of the two peaks significantly decreased. Hereafter, with further increasing the number of ALD cycles, the intensity of the peak at 504 nm slightly lowered, while the change of the peak at 385 nm was insignificant. It is known that the lower PL intensity reflects the lower recombination rate of the photogenerated charge carriers [89,90]. Therefore, this indicates that the coating of SiO_2 has improved charge separation, which consequently enhanced the photocatalytic activity of TiO_2. This was also observed for the TiO_2/SiO_2 core/shell photocatalysts synthesized by sol–gel method reported by Yuan et al. [51]. According to Yuan et al, the enhancement of charge carrier separation is due to the formation of Ti–O–Si bonds at the interface between TiO_2 and SiO_2, which is also evidenced from the XPS spectra shown in Fig. 3.

4. Conclusions

In conclusion, ALD using $SiCl_4$ and H_2O carried out in a fluidized bed reactor operating at atmospheric pressure enabled the deposition of

SiO_2 on P25 TiO_2 nanoparticles at 100 °C, which is significantly lower than the deposition temperature in conventional ALD processes. With a growth-per-cycle of 0.5 Å, the ALD process provided the ability to control the thickness of the SiO_2 layer at the sub-nanometer level, which allowed us to study the influence of the coating thickness on the photocatalytic activity of the TiO_2/SiO_2 on the degradation of RhB solution under UV-light irradiation. We observed that the coating of SiO_2 with a thickness of below 1.4 nm provided a considerable photocatalytic activity enhancement, whereas at a thickness of above 1.4 nm, the photocatalytic activity was strongly suppressed. The photocatalytic activity enhancement is attributed to the improved charge separation facilitated by the Ti–O–Si bonds that are formed at the interface between TiO_2 and SiO_2. As the thickness of SiO_2 layer increases, the SiO_2 layer inhibits the charge transport from TiO_2 to the outer surface, which consequently suppresses the photocatalytic activity. With the aid of using carrier and radical scavengers, namely, EDTA as the hole scavenger, DMSO as the OH· radical scavenger and benzoquinone as the H_2O_2 scavenger, we found that OH· radicals were the main oxidizing species for degradation of RhB solution.

In addition, the obtained results have shown that by controlling the thickness of the SiO_2 layer in a very narrow range, i.e., below 2 nm, the photocatalytic property of TiO_2 can be altered from enhancement to suppression. Therefore, our work has demonstrated a feasible and efficient route not only for the synthesis of noble-metal free TiO_2-based photocatalysts with an enhanced activity, but also for tuning the photocatalytic properties. Moreover, the low-temperature ALD process is an important asset which can enable the application of SiO_2 coating on temperature-sensitive materials such as polymers and organic materials.

Declaration of Competing Interest

The authors declare that they have no known competing financial interests or personal relationships that could have appeared to influence the work reported in this paper.

Acknowledgements

The authors acknowledge Willy Rook (Catalysis Engineering, ChemE, Delft University of Technology) for the BET characterizations. Mehmet Sarilar and Baukje Terpstra (Reactor Institute of Delft University of Technology) are acknowledged for the INAA measurements and analyses. Jing Guo acknowledges the financial support from the National Natural Science Foundation of China (Project number 21808214). Dominik Benz acknowledges the financial support from the Delft Global Initiative. Hao Van Bui acknowledges the financial support from Vietnam National Foundation for Science and Technology Development (NAFOSTED) under grant number 103.02-2017.373.

Appendix A. Supplementary data

Supplementary data to this article can be found online at https://doi.org/10.1016/j.apsusc.2020.147244.

References

[1] A. Fujishima, K. Honda, Electrochemical photolysis of water at a semiconductor electrode, Nature 238 (1972) 37–38, https://doi.org/10.1038/238037a0.
[2] K. Nakata, A. Fujishima, TiO_2 photocatalysis: design and applications, J. Photochem. Photobiol. C Photochem. Rev. 13 (2012) 169–189, https://doi.org/10.1016/j.jphotochemrev.2012.06.001.
[3] L.G. Devi, R. Kavitha, A review on non metal ion doped titania for the photocatalytic degradation of organic pollutants under UV/solar light: Role of photogenerated charge carrier dynamics in enhancing the activity, Appl. Catal. B, Environ. 140–141 (2013) 559–587. https://doi.org/10.1016/j.apcatb.2013.04.035.
[4] P. Ganguly, C. Byrne, A. Breen, S.C. Pillai, Antimicrobial activity of photocatalysts: fundamentals, mechanisms, kinetics and recent advances, Appl. Catal. B, Environ. 225 (2018) 51–75, https://doi.org/10.1016/j.apcatb.2017.11.018.
[5] M. Motegh, J.R. Van Ommen, P.W. Appel, M.T. Kreutzer, Scale-up study of a multiphase photocatalytic reactor: degradation of cyanide in water over TiO_2, Environ. Sci. Technol. 48 (2014) 1574–1581, https://doi.org/10.1021/es403378e.
[6] J. Schneider, M. Matsuoka, M. Takeuchi, J. Zhang, Y. Horiuchi, M. Anpo, D.W. Bahnemann, Understanding TiO_2 photocatalysis: mechanisms and materials, Chem. Rev. 114 (2014) 9919–9986, https://doi.org/10.1021/cr5001892.
[7] X. Chen, S.S. Mao, Titanium dioxide nanomaterials: synthesis, properties, modifications and applications, Chem. Rev. 107 (2007) 2891–2959, https://doi.org/10.1021/cr0500535.
[8] S.G. Kumar, L.G. Devi, Review on modified TiO_2 photocatalysis under UV/visible light: selected results and related mechanisms on interfacial charge carrier transfer dynamics, J. Phys. Chem. A 115 (2011) 13211–13241, https://doi.org/10.1021/jp204364a.
[9] B. Ohtani, Titania photocatalysis beyond recombination: a critical review, Catalysts. 3 (2013) 942–953, https://doi.org/10.3390/catal3040942.
[10] S. Chang, W. Liu, The roles of surface-doped metal ions (V, Mn, Fe, Cu, Ce, and W) in the interfacial behavior of TiO2 photocatalysts, Appl. Catal. B, Environ. 156–157 (2014) 466–475. https://doi.org/10.1016/j.apcatb.2014.03.044.
[11] O. Elbanna, P. Zhang, M. Fujitsuka, T. Majima, Facile preparation of nitrogen and fluorine codoped TiO_2 mesocrystal with visible light photocatalytic activity, Appl. Catal. B, Environ. 192 (2016) 80–87, https://doi.org/10.1016/j.apcatb.2016.03.053.
[12] A.E. Giannakas, M. Antonopoulou, C. Daikopoulos, Y. Deligiannakis, Characterization and catalytic performance of B-doped , B – N co-doped and B – N – F tri-doped TiO2 towards simultaneous Cr (VI) reduction and benzoic acid oxidation, Appl. Catal. B, Environ. 184 (2016) 44–54. https://doi.org/10.1016/j.apcatb.2015.11.009.
[13] S. Nagi, R. Inturi, T. Boningari, M. Suidan, P.G. Smirniotis, Visible-light-induced photodegradation of gas phase acetonitrile using aerosol-made transition metal (V, Cr, Fe, Co, Mn, Mo, Ni, Cu, Y, Ce, and Zr) doped TiO2, Appl. Catal. B, Environ. 144 (2013) 333–342. https://doi.org/10.1016/j.apcatb.2013.07.032.
[14] H. Park, Y. Park, W. Kim, W. Choi, Surface modification of TiO_2 photocatalyst for environmental applications, J. Photochem. Photobiol. C Photochem. Rev. 15 (2013) 1–20, https://doi.org/10.1016/j.jphotochemrev.2012.10.001.
[15] R. Asahi, T. Morikawa, T. Ohwaki, K. Aoki, Y. Taga, Visible-light photocatalysis in nitrogen-doped titanium oxides, Science (80-.). 293 (2001) 269–271. https://doi.org/10.1126/science.1061051.
[16] R. Asahi, T. Morikawa, H. Irie, T. Ohwaki, Nitrogen-doped titanium dioxide as visible-light-sensitive photocatalyst: designs, developments, and prospects, Chem. Rev. 114 (2014) 9824–9852, https://doi.org/10.1021/cr5000738.
[17] M. Tahir, B. Tahir, N. Aishah, S. Amin, Synergistic effect in plasmonic Au/Ag alloy NPs co-coated TiO_2 NWs toward visible-light enhanced CO_2 photoreduction to fuels, Appl. Catal. B, Environ. 204 (2017) 548–560, https://doi.org/10.1016/j.apcatb.2016.11.062.
[18] Z. Wei, M. Janczarek, K. Maya Endo, Wang, A. Balcytis, M.G.M.-M. Akio Nitta, S.J. Christophe Colbeau-Justin, B. Ohtani, E. Kowalska, Noble metal-modified faceted anatase titania photocatalysts: Octahedron versus decahedron, Appl. Catal. B, Environ. 237 (2018) 574–587. https://doi.org/10.1016/j.apcatb.2018.06.027.
[19] A. Maria, V. Dozzi, G.L. Chiarello, S. Livraghi, E. Giamello, E. Selli, High photocatalytic hydrogen production on Cu(II) pre-grafted Pt/TiO_2, Appl. Catal. B, Environ. 209 (2017) 417–428, https://doi.org/10.1016/j.apcatb.2017.03.007.
[20] L. Collado, A. Reynal, J.M. Coronado, D.P. Serrano, J.R. Durrant, V.A.P. de laO'Shea, Effect of Au surface plasmon nanoparticles on the selective CO_2 photoreduction to CH_4, Appl. Catal. B, Environ. 178 (2014) 177–185, https://doi.org/10.1016/j.apcatb.2014.09.032.
[21] S. Xie, Y. Wang, Q. Zhang, W. Fan, W. Deng, Y. Wang, Photocatalytic reduction of CO_2 with H_2O: significant enhancement of the activity of $Pt–TiO_2$ in CH_4 formation by addition of MgO, Chem. Commun. 49 (2013) 2451–2453, https://doi.org/10.1039/c3cc00107e.
[22] M. Jakob, H. Levanon, P.V. Kamat, Charge distribution between UV-irradiated TiO_2 and gold nanoparticles: Determination of shift in the Fermi level, Nano Lett. 3 (2003) 353–358, https://doi.org/10.1021/nl0340071.
[23] V. Subramanian, E.E. Wolf, P.V. Kamat, Catalysis with TiO_2/gold nanocomposites. Effect of metal particle size on the Fermi level equilibration, J. Am. Chem. Soc. 126 (2004) 4943–4950, https://doi.org/10.1021/ja0315199.
[24] J.R. Van Ommen, D. Kooijman, M. De Niet, M. Talebi, A. Goulas, Continuous production of nanostructured particles using spatial atomic layer deposition, J. Vac. Sci. Technol. A Vacuum, Surfaces, Film. 33 (2015) 021513, , https://doi.org/10.1116/1.4905725.
[25] M.G. Méndez-Medrano, E. Kowalska, A. Lehoux, A. Herissan, B. Ohtani, D. Bahena, V. Briois, C. Colbeau-Justin, J.L. Rodríguez-López, H. Remita, Surface modification of TiO_2 with Ag nanoparticles and CuO nanoclusters for application in photocatalysis, J. Phys. Chem. C 120 (2016) 5143–5154, https://doi.org/10.1021/acs.jpcc.5b10703.
[26] T. Wang, J. Wei, H. Shi, M. Zhou, Y. Zhang, Q. Chen, Z. Zhang, Preparation of electrospun Ag/TiO_2 nanotubes with enhanced photocatalytic activity based on water/oil phase separation, Phys. E Low-Dimensional Syst. Nanostructures. 86 (2017) 103–110, https://doi.org/10.1016/j.physe.2016.10.016.
[27] M.K. Kumar, K. Bhavani, G. Naresh, B. Srinivas, A. Venugopal, Plasmonic resonance nature of $Ag-Cu/TiO_2$ photocatalyst under solar and artificial light: Synthesis, characterization and evaluation of H_2O splitting activity, Appl. Catal. B, Environ. 199 (2016) 282–291, https://doi.org/10.1016/j.apcatb.2016.06.050.
[28] V. Subramanian, E. Wolf, P.V. Kamat, Semiconductor-metal composite nanostructures. To what extent do metal nanoparticles improve the photocatalytic activity of TiO_2 films? J. Phys. Chem. B 105 (2001) 11439–11446, https://doi.org/10.1021/jp011118k.

[29] Y. Wang, J. Zhao, T. Wang, Y. Li, X. Li, J. Yin, C. Wang, CO_2 photoreduction with H_2O vapor on highly dispersed CeO_2/TiO_2 catalysts: surface species and their reactivity, J. Catal. 337 (2016) 293–302, https://doi.org/10.1016/j.jcat.2015.12.030.

[30] M. Stucchi, D.C. Boffito, E. Pargoletti, C.L. Bianchi, G. Cappelletti, Nano-MnO_2 decoration of TiO_2 microparticles to promote gaseous ethanol visible photoremoval, Nanomaterials 8 (2018) 686, https://doi.org/10.3390/nano8090686.

[31] S. Xie, Y. Wang, Q. Zhang, W. Deng, Y. Wang, MgO- and Pt-promoted TiO_2 as an efficient photocatalyst for the preferential reduction of carbon dioxide in the presence of water, ACS Catal. 4 (2014) 3644–3653, https://doi.org/10.1021/cs500648p.

[32] S.J.A. Moniz, S.A. Shevlin, X. An, Z.X. Guo, J. Tang, Fe_2O_3-TiO_2 nanocomposites for enhanced charge separation and photocatalytic activity, Chem. – A Eur. J. 20 (2014) 15571–15579, https://doi.org/10.1002/chem.201403489.

[33] L. Tsui, G. Zangari, Modification of TiO_2 nanotubes by Cu_2O for photoelectrochemical, photocatalytic, and photovoltaic devices, Electrochim. Acta 128 (2013) 341–348, https://doi.org/10.1016/j.electacta.2013.09.150.

[34] K. Zhao, S. Zhao, J. Qi, H. Yin, C. Gao, A.M. Khattak, Y. Wu, A. Iqbal, L. Wu, Y. Gao, R. Yu, Z. Tang, Cu_2O clusters grown on TiO_2 nanoplates as efficient photocatalysts for hydrogen generation, Inorg. Chem. Front. 3 (2016) 488–493, https://doi.org/10.1039/c5qi00284b.

[35] J. Guo, S. Yuan, Y. Yu, J.R. van Ommen, H. Van Bui, B. Liang, Room-temperature pulsed CVD-grown SiO_2 protective layer on TiO_2 particles for photocatalytic activity suppression, RSC Adv. 7 (2017) 4547–4554, https://doi.org/10.1039/c6ra27976g.

[36] X. Liang, K.S. Barrett, Y.B. Jiang, A.W. Weimer, Rapid silica atomic layer deposition on large quantities of cohesive nanoparticles, ACS Appl. Mater. Interfaces 2 (2010) 2248–2253, https://doi.org/10.1021/am100279v.

[37] D.M. King, X. Liang, B.B. Burton, M. Kamal Akhtar, A.W. Weimer, Passivation of pigment-grade TiO_2 particles by nanothick atomic layer deposited SiO_2 films, Nanotechnology 19 (2008) 2248–2253, https://doi.org/10.1088/0957-4484/19/25/255604.

[38] A. Šuligoj, U.L. Štangar, A. Ristić, M. Mazaj, D. Verhovšek, N.N. Tušar, TiO_2-SiO_2 films from organic-free colloidal TiO_2 anatase nanoparticles as photocatalyst for removal of volatile organic compounds from indoor air, Appl. Catal. B Environ. 184 (2016) 119–131, https://doi.org/10.1016/j.apcatb.2015.11.007.

[39] C. Anderson, A.J. Bard, An improved photocatalyst of TiO_2/SiO_2 prepared by a sol-gel synthesis, J. Phys. Chem. 99 (1995) 9882–9885, https://doi.org/10.1021/j100024a033.

[40] G. Li, F. Liu, Z. Zhang, Enhanced photocatalytic activity of silica-embedded TiO_2 hollow microspheres prepared by one-pot approach, J. Alloy. Compd. 493 (2010) L1–L7, https://doi.org/10.1016/j.jallcom.2009.12.046.

[41] J. Aguado, R. van Grieken, M.J. López-Muñoz, J. Marugán, A comprehensive study of the synthesis, characterization and activity of TiO_2 and mixed TiO_2/SiO_2 photocatalysts, Appl. Catal. A Gen. 312 (2006) 202–212, https://doi.org/10.1016/j.apcata.2006.07.003.

[42] B. Malinowska, J. Walendziewski, D. Robert, J.V. Weber, M. Stolarski, The study of photocatalytic activities of titania and titania-silica aerogels, Appl. Catal. B Environ. 46 (2003) 441–451, https://doi.org/10.1016/S0926-3373(03)00273-X.

[43] H.R. Jafry, M.V. Liga, Q. Li, A.R. Barron, Simple route to enhanced photocatalytic activity of P25 titanium dioxide nanoparticles by silica addition, Environ. Sci. Technol. 45 (2011) 1563–1568, https://doi.org/10.1021/es102749e.

[44] S. Yaparatne, C.P. Tripp, A. Amirbahman, Photodegradation of taste and odor compounds in water in the presence of immobilized TiO_2-SiO_2 photocatalysts, J. Hazard. Mater. 346 (2018) 208–217, https://doi.org/10.1016/j.jhazmat.2017.12.029.

[45] G. Li, K.A. Gray, The solid-solid interface: explaining the high and unique photocatalytic reactivity of TiO_2-based nanocomposite materials, Chem. Phys. 339 (2007) 173–187, https://doi.org/10.1016/j.chemphys.2007.05.023.

[46] C. Kang, L. Jing, T. Guo, H. Cui, J. Zhou, H. Fu, Mesoporous SiO_2-modified nanocrystalline TiO_2 with high anatase thermal stability and large surface area as efficient photocatalyst, J. Phys. Chem. C 113 (2009) 1006–1013, https://doi.org/10.1021/jp807552u.

[47] Y. Yu, M. Zhu, W. Liang, S. Rhodes, J. Fang, Synthesis of silica–titania composite aerogel beads for the removal of Rhodamine B in water, RSC Adv. 5 (2015) 72437–72443, https://doi.org/10.1039/C5RA13625C.

[48] I. Levchuk, M. Kralova, J.J. Rueda-Márquez, J. Moreno-Andrés, S. Gutiérrez-Alfaro, P. Dzik, S. Parola, M. Sillanpää, R. Vahala, M.A. Manzano, Antimicrobial activity of printed composite TiO_2/SiO_2 and TiO_2/SiO_2/Au thin films under UVA-LED and natural solar radiation, Appl. Catal. B, Environ. 239 (2018) 609–618, https://doi.org/10.1016/j.apcatb.2018.08.051.

[49] M.V. Liga, S.J. Maguire-Boyle, H.R. Jafry, A.R. Barron, Q. Li, Silica decorated TiO_2 for virus inactivation in drinking water -simple synthesis method and mechanisms of enhanced inactivation kinetics, Environ. Sci. Technol. 47 (2013) 6463–6470, https://doi.org/10.1021/es400196p.

[50] F.A. Harraz, O.E. Abdel-Salam, A.A. Mostafa, R.M. Mohamed, M. Hanafy, Rapid synthesis of titania-silica nanoparticles photocatalyst by a modified sol-gel method for cyanide degradation and heavy metals removal, J. Alloy. Compd. 551 (2013) 1–7, https://doi.org/10.1016/j.jallcom.2012.10.004.

[51] L. Yuan, C. Han, M. Pagliaro, Y. Xu, Origin of enhancing the photocatalytic performance of TiO_2 for artificial photoreduction of CO_2 through a SiO_2 coating strategy, J. Phys. Chem. C 120 (2016) 265–273, https://doi.org/10.1021/acs.jpcc.5b08893.

[52] E.P. Ferreira-Neto, S. Ullah, M.B. Simões, A.P. Perissinotto, F.S. de Vicente, P.L.M. Noeske, S.J.L. Ribeiro, U.P. Rodrigues-Filho, Solvent-controlled deposition of titania on silica spheres for the preparation of SiO_2@TiO_2 core@shell nanoparticles with enhanced photocatalytic activity, Colloids Surfaces A Physicochem. Eng. Asp. 570 (2019) 293–305, https://doi.org/10.1016/j.colsurfa.2019.03.036.

[53] J. Yang, X. Xu, Y. Liu, Y. Gao, H. Chen, H. Li, Preparation of SiO_2@TiO_2 composite nanosheets and their application in photocatalytic degradation of malachite green at emulsion interface, Colloids Surfaces A Physicochem. Eng. Asp. 582 (2019) 123858, , https://doi.org/10.1016/j.colsurfa.2019.123858.

[54] W. Wang, H. Chen, J. Fang, M. Lai, Large-scale preparation of rice-husk-derived mesoporous SiO_2@TiO_2 as efficient and promising photocatalysts for organic contaminants degradation, Appl. Surf. Sci. 467–468 (2019) 1187–1194, https://doi.org/10.1016/j.apsusc.2018.10.275.

[55] Q. Wu, C. Liu, J. Peng, F. Liu, New insights into high temperature hydrothermal synthesis in the preparation of visible-light active, ordered mesoporous SiO_2-TiO_2 composited photocatalysts, RSC Adv. 7 (2017) 19557–19564, https://doi.org/10.1039/c7ra01368j.

[56] Z. Li, B. Hou, Y. Xu, D. Wu, Y. Sun, Hydrothermal synthesis, characterization, and photocatalytic performance of silica-modified titanium dioxide nanoparticles, J. Colloid Interface Sci. 288 (2005) 149–154, https://doi.org/10.1016/j.jcis.2005.02.082.

[57] X. Gao, I.E. Wachs, Titania-silica as catalysts: Molecular structural characteristics and physico-chemical properties, Catal. Today 51 (1999) 233–254, https://doi.org/10.1016/S0920-5861(99)00048-6.

[58] D.J. Simpson, A. Thilagam, G.P. Cavallaro, K. Kaplun, A.R. Gerson, SiO_2 coated pure and doped titania pigments: Low temperature CVD deposition and quantum chemical study, PCCP 13 (2011) 21132–21138, https://doi.org/10.1039/c1cp22681a.

[59] H. Van Bui, F. Grillo, J.R. van Ommen, Atomic and molecular layer deposition: off the beaten track, Chem. Commun. 53 (2017) 45–71, https://doi.org/10.1039/c6cc05568k.

[60] R.L. Puurunen, Surface chemistry of atomic layer deposition: a case study for the trimethylaluminum/water process, J. Appl. Phys. 97 (2005) 121301, , https://doi.org/10.1063/1.1940727.

[61] J. Guo, H. Van Bui, D. Valdesueiro, S. Yuan, B. Liang, J.R. van Ommen, Suppressing the photocatalytic activity of TiO_2 nanoparticles by extremely thin Al_2O_3 films grown by gas-phase deposition at ambient conditions, Nanomaterials. 8 (2018) 61, https://doi.org/10.3390/nano8020061.

[62] J.D. Ferguson, A.W. Weimer, S.M. George, Atomic layer deposition of SiO_2 films on BN particles using sequential surface reactions, Chem. Mater. 12 (2000) 3472–3480, https://doi.org/10.1021/cm000313t.

[63] O. Sneh, M.L. Wise, A.W. Ott, L.A. Okada, S.M. George, Atomic layer growth of SiO_2 on Si(100) using $SiCl_4$ and H_2O in a binary reaction sequence, Surf. Sci. 334 (1995) 135–152, https://doi.org/10.1016/0039-6028(95)00471-8.

[64] J.K. Kang, C.B. Musgrave, Mechanism of atomic layer deposition of SiO_2 on the silicon (100)-2×1 surface using $SiCl_4$ and H_2O as precursors, J. Appl. Phys. 91 (2002) 3408, https://doi.org/10.1063/1.1436294.

[65] J.W. Klaus, S.M. George, SiO_2 chemical vapor deposition at room temperature using $SiCl_4$ and H_2O with an NH_3 catalyst, J. Electrochem. Soc. 147 (2000) 2658–2664, https://doi.org/10.1149/1.1393586.

[66] Y. Du, X. Du, S.M. George, SiO_2 film growth at low temperatures by catalyzed atomic layer deposition in a viscous flow reactor, Thin Solid Films 491 (2005) 43–53, https://doi.org/10.1016/j.tsf.2005.05.051.

[67] J.H. de Boer, B.C. Lippens, B.G. Linsen, J.C.P. Broekhoff, A. van den Heuvel, T.J. Osinga, The t-curve of multimolecular N_2-adsorption, J. Colloid Interface Sci. 21 (1966) 405–414, https://doi.org/10.1016/0095-8522(66)90006-7.

[68] J. Jun, M. Dhayal, J.H. Shin, J.C. Kim, N. Getoff, Surface properties and photoactivity of TiO_2 treated with electron beam, Radiat. Phys. Chem. 75 (2006) 583–589, https://doi.org/10.1016/j.radphyschem.2005.10.015.

[69] M.C. Biesinger, B.P. Payne, A.P. Grosvenor, L.W.M. Lau, A.R. Gerson, R.S.C. Smart, Resolving surface chemical states in XPS analysis of first row transition metals, oxides and hydroxides: Cr, Mn, Fe, Co and Ni, Appl. Surf. Sci. 257 (2011) 2717–2730, https://doi.org/10.1016/j.apsusc.2010.10.051.

[70] A. Sasahara, C.L. Pang, M. Tomitori, Atomic scale analysis of ultrathin SiO_2 films prepared on TiO_2(100) surfaces, J. Phys. Chem. C 114 (2010) 20189–20194, https://doi.org/10.1021/jp108380r.

[71] S.S. Chao, Y. Takagi, G. Lucovsky, P. Pai, R.C. Custer, J.E. Tyler, J.E. Keem, Chemical states study of Si in SiOx films grown by PECVD, Appl. Surf. Sci. 26 (1986) 575–583, https://doi.org/10.1016/0169-4332(86)90128-5.

[72] Y. Xu, Z. Zeng, The preparation, characterization, and photocatalytic activities of Ce-TiO_2/SiO_2, J. Mol. Catal. A: Chem. 279 (2008) 77–81, https://doi.org/10.1016/j.molcata.2007.09.016.

[73] S. Ren, X. Zhao, L. Zhao, M. Yuan, Y. Yu, Y. Guo, Z. Wang, Preparation of porous TiO_2/silica composites without any surfactants, J. Solid State Chem. 182 (2009) 312–316, https://doi.org/10.1016/j.jssc.2008.10.027.

[74] H. Zhang, X. Luo, J. Xu, B. Xiang, D. Yu, Synthesis of TiO_2/SiO_2 core/shell nanocable arrays, J. Phys. Chem. B 108 (2004) 14866–14869, https://doi.org/10.1021/jp049770d.

[75] C. Anderson, A.J. Bard, Improved photocatalytic activity and characterization of mixed TiO_2/SiO_2 and TiO_2/Al_2O_3 materials, J. Phys. Chem. B 101 (1997) 2611–2616, https://doi.org/10.1021/jp9626982.

[76] S. Wang, F. Teng, Y. Zhao, Effect of the molecular structure and surface charge of a bismuth catalyst on the adsorption and photocatalytic degradation of dye mixtures, RSC Adv. 5 (2015) 76588–76598, https://doi.org/10.1039/C5RA14931B.

[77] A. Fujishima, X. Zhang, D.A. Tryk, TiO_2 photocatalysis and related surface phenomena, Surf. Sci. Rep. 63 (2008) 515–582, https://doi.org/10.1016/j.surfrep.2008.10.001.

[78] M. Auffan, M. Pedeutour, J. Rose, A. Masion, F. Ziarelli, D. Borschneck, C. Chaneac, C. Botta, P. Chaurand, J. Labille, J.Y. Bottero, Structural degradation at the surface of a TiO_2-based nanomaterial used in cosmetics, Environ. Sci. Technol. 44 (2010)

2689–2694, https://doi.org/10.1021/es903757q.
[79] Y. Nosaka, A. Nosaka, Understanding hydroxyl radical (•OH) generation processes in photocatalysis, ACS Energy Lett. 1 (2016) 356–359, https://doi.org/10.1021/acsenergylett.6b00174.
[80] Y. Nosaka, A.Y. Nosaka, Generation and detection of reactive oxygen species in photocatalysis, Chem. Rev. 117 (2017) 11302–11336, https://doi.org/10.1021/acs.chemrev.7b00161.
[81] T. Hirakawa, K. Yawata, Y. Nosaka, Photocatalytic reactivity for O_2- and OH radical formation in anatase and rutile TiO_2 suspension as the effect of H_2O_2 addition, Appl. Catal. A Gen. 325 (2007) 105–111, https://doi.org/10.1016/j.apcata.2007.03.015.
[82] J. Zhang, Y. Nosaka, Mechanism of the OH radical generation in photocatalysis with TiO_2 of different crystalline types, J. Phys. Chem. C 118 (2014) 10824–10832, https://doi.org/10.1021/jp501214m.
[83] C.S. Turchi, D.F. Ollis, Photocatalytic degradation of organic water contaminants: mechanisms involving hydroxyl radical attack, J. Catal. 122 (1990) 178–192, https://doi.org/10.1016/0021-9517(90)90269-P.
[84] T. Liu, L. Wang, X. Lu, J. Fan, X. Cai, B. Gao, R. Miao, J. Wang, Y. Lv, Comparative study of the photocatalytic performance for the degradation of different dyes by $ZnIn_2S_4$: adsorption, active species, and pathways, RSC Adv. 7 (2017) 12292–12300, https://doi.org/10.1039/c7ra00199a.
[85] M. Pelaez, P. Falaras, V. Likodimos, K. O'Shea, A.A. de la Cruz, P.S.M. Dunlop, J.A. Byrne, D.D. Dionysiou, Use of selected scavengers for the determination of NF-TiO_2 reactive oxygen species during the degradation of microcystin-LR under visible light irradiation, J. Mol. Catal. A: Chem. 425 (2016) 183–189, https://doi.org/10.1016/j.molcata.2016.09.035.
[86] X.H. Lin, Y. Miao, F.Y. Li, Location of photocatalytic oxidation processes on anatase titanium dioxide, Catal. Sci. Technol. 7 (2017) 441–451, https://doi.org/10.1039/c6cy02214f.
[87] J. Xu, L. Li, Y. Yan, H. Wang, X. Wang, X. Fu, G. Li, Synthesis and photoluminescence of well-dispersible anatase TiO_2 nanoparticles, J. Colloid Interface Sci. 318 (2008) 29–34, https://doi.org/10.1016/j.jcis.2007.10.004.
[88] D.K. Pallotti, L. Passoni, P. Maddalena, F. Di Fonzo, S. Lettieri, Photoluminescence mechanisms in anatase and rutile TiO_2, J. Phys. Chem. C 121 (2017) 9011–9021, https://doi.org/10.1021/acs.jpcc.7b00321.
[89] L. Yuan, M. Yang, Y. Xu, A low-temperature and one-step method for fabricating $ZnIn_2S_4$–GR nanocomposites with, J. Mater. Chem. A 2 (2014) 14401–14412, https://doi.org/10.1039/C4TA02670E.
[90] C. Han, M.Q. Yang, N. Zhang, Y.J. Xu, Enhancing the visible light photocatalytic performance of ternary CdS-(graphene-Pd) nanocomposites via a facile interfacial mediator and co-catalyst strategy, J. Mater. Chem. A 2 (2014) 19156–19166, https://doi.org/10.1039/c4ta04151h.